"A Cochlear Nucleus Auditory prosthesis based on microstimulation"

Contract No. NO1-DC-8-2102
QUARTERLY PROGRESS REPORT #4
April 1, 1999-June 30, 1999

HUNTINGTON MEDICAL RESEARCH INSTITUTES
NEUROLOGICAL RESEARCH LABORATORY
734 Fairmount Avenue
Pasadena, California 91105

D.B. McCreery, Ph.D.
W.F. Agnew, Ph.D.
T.G.H. Yuen, Ph.D.
L.A. Bullara, B.S.

HOUSE EAR INSTITUTE
2100 WEST THIRD STREET
Los Angeles, California 90057

Robert Shannon, Ph.D
Jean Moore, Ph.D
Steve Otto. M.S.

ABSTRACT AND SUMMARY

These studies are a continuation of our program to determine safe and effective stimulus parameters for an auditory prosthesis based on multisite microstimulation in the ventral cochlear nucleus. We report on three ongoing studies. In one study (conducted in cat CN133) we attempted to reduce the severity of the stimulation-induced depression of neuronal excitability (SIDNE) that develops during prolonged intranuclear microstimulation. Our technique was to gradually increase the stimulus frequency over a span of 30 days. This conditioning regimen did not reduce the SIDNE near the response threshold. However, data from this animals did suggest that SIDNE, and also short-acting refractory phenomena (analogous to forward-masking) might be ameliorated by distributing the stimulation over a larger number of electrode sites, and pulsing each site at a lower rate. In the second study, cats CN130 and CN133 were used to evaluate the safety and efficacy of prolonged stimulation using short-duration (40 μs/ph), high-amplitude (high current density) stimulus pulses. In cat CN130, in which the microelectrodes' geometric surface area was approximately 1,000 μm^2, pulsing the microelectrodes for 7 hours per day for 11 days, using a protocol in which the stimulus amplitude reached 63 μA (2.5 nC/phase), did not induce histologically-detectable injury to the nearby neurons or neuropil, but there was some evidence that the prolonged, high amplitude stimulation induced some additional gliosis near the electrode tips. Also, the threshold of the evoked response increased slightly throughout the 11 days of stimulation. In cat CN133, in which the electrodes' surface area was larger (approximately 2,000 μm^2) the thresholds of the evoked response was stable after the first day (7 hours) of stimulation and there was no evidence of active gliosis near the electrode tips.

We also conducted a special test in which one iridium microelectrode was permanently connected to the platinum ground electrode, for 61 days. This treatment did not induce any detectable histologic changes near the electrode tip, and the threshold of the evoked response, and the slope of its recruitment curve, remained unchanged throughout the 61 days.

INTRODUCTION

We present the results from 2 cats in which arrays of 4 iridium microelectrodes had been implanted chronically into the posteroventral cochlear nucleus. Three separate studies were conducted in these 2 animals, and the studies were sequenced so as to interact as little as possible. In one study conducted in cat CN133, we attempted to reduce the severity of the stimulation-induced depression of neuronal excitability (SIDNE) that develops during prolonged intranuclear microstimulation. Our technique was to gradually increase the stimulus frequency over a span of 30 days.

In the second study, cats CN130 and CN133 were used to evaluate the safety and efficacy of prolonged stimulation using short-duration (40 μs/ph), high-amplitude (high current density) stimulus pulses. This pulsing protocol is compatible with the circuitry in the existing clinical stimulators (which were designed to drive macroelectrodes, rather than microelectrodes). Cat CN133 is the first of 3 animals in which we are evaluating the merits of using electrodes with somewhat larger surface areas (2,000 μm^2) in order to reduce the current density at the electrode-tissue interface.

The third study (conducted with Cat CN130) was to determine if there are hazards associated with permanently shorting an iridium microelectrode to a platinum ground. This situation will arise when the array of penetrating iridium microelectrodes is integrated with the array of platinum surface electrodes used in the present auditory brainstem implant, and both arrays are driven by the Cochlear Corporation CI24M sound processor/stimulator.

METHODS

Fabrication of stimulating microelectrodes.

Activated iridium stimulating microelectrodes are fabricated from lengths of pure iridium wire, 50 μm in diameter. A Teflon-insulated lead wire is welded to one end of the iridium shaft, and the other end is shaped to a conical taper, by electrolytic etching. The microelectrodes have relatively blunt tips (a radius of curvature of approximately 6 μm) to reduce tissue injury during insertion into the brain, and to allow better distribution of

the stimulus current over the exposed surface area. The entire shaft and wire junction then is coated with 3 thin layers of Epoxylite 6001-50 heat-cured electrode varnish. The insulation is removed from the tip by ablation with an erbium laser, leaving an exposed geometric surface area of 1000 +/- 150 μm^2 or 2000 +/- 300 μm^2. The individual electrodes are assembled into an integrated array of 4 microelectrodes spaced approximately 400 μm apart. The integrated array, with its closely-spaced microelectrode shafts, is designed to approximate the dimensions of an array that can be implanted into the human posteroventral cochlear nucleus using a tool inserted through the translabyrinthine surgical approach to the CP angle.

The iridium electrodes are "activated" to increase their charge capacities, then soaked in deionized water for 120 hours, and sterilized with ethylene oxide.

Implantation of stimulating and recording electrodes

Young adult cats are anesthetized with Pentothal sodium, with transition to a mixture of nitrous oxide and Halothane. Implantation of the electrodes is conducted using aseptic surgical technique. The cat's head is placed in a stereotaxic frame, and the skull is exposed as far back as the posterior fossa by reflecting the scalp and muscles. A pair of stainless steel recording electrodes is implanted by stereotaxis into the right inferior colliculus through a small craniectomy. The compound action potential induced by a train of clicks delivered to the left ear is used to position the recording electrodes.

A small craniectomy is made over the cerebellum, through which the array of iridium stimulating electrodes is inserted by stereotaxis into the left posteroventral cochlear nucleus (PVCN). The array of microelectrodes was inserted through a portion of the overlying cerebellar flocculus, so that we could evaluate electrodes whose length was appropriate for use in humans. The microelectrodes were positioned first by stereotaxic coordinates and the final positioning was achieved by observing the compound potential evoked in the inferior colliculus while stimulating with the microelectrode.

Stimulation protocols and data acquisition

For the prolonged stimulation regimen, we have simulated an acoustic environment with a computer-generated artificial voice, which reproduces many of the characteristics of real speech, including the long-term average spectrum, the short-term spectrum, the instantaneous amplitude distribution, the voiced and unvoiced structure of speech, and the syllabic envelope. This signal was developed by the International Telegraphic & Telephony Consultive Convention (CCITT) for testing telecommunication equipment. In addition to the computer-generated artificial voice, the signal contains added noise, at approximately 16 decibels below the mean level of the voice. The artificial voice signal is passed through a full-wave rectifier and then undergoes logarithmic amplitude compression, before being sent through an appropriate anti-aliasing filter. The amplitude of the filtered signal modulates the amplitude of the charge-balanced stimulus pulses which are delivered to each electrode at 100- 250 Hz, in an interleaved manner. Our model system differs slightly from that which would occur in a clinical speech processor, in that we have not partitioned the signal into bands, according to acoustic frequency composition. In our system, the same signal is sent to all of the microelectrodes, in an interleaved mode. The range of spike amplitudes is shifted so that acoustic silence is mapped to a stimulus amplitude which is close to the response threshold of the neurons near the tip of the properly functioning microelectrodes (14 μA when the stimulus pulse duration is 40 μs/phase). Figure 1 shows the amplitude distribution of the stimulus pulses that have been amplitude-modulated according to the logarithmically-compressed artificial voice signal. Note that the logarithmic amplitude compression has caused the pulse amplitudes to be clustered at the upper end of the amplitude range.

The artificial voice signal was presented for 15 seconds followed by 15 seconds in which the stimulus amplitude was held near the threshold of the evoked response. This 50% duty cycle is intended to simulate a moderately noisy acoustic environment. Stimulation and data acquisition was conducted using the two-way radiotelemetry stimulation and data acquisition system described previously. This telemetry system and its companion software allows continuous monitoring of the voltage waveform

across the stimulating microelectrodes, and of the compound evoked potential induced in the inferior colliculus by the stimulating microelectrodes.

Before and after each daily session of stimulation, the recruitment curves of the evoked responses were recorded in the inferior colliculus. The responses evoked by 1024 to 4096 consecutive charge-balanced, controlled-current stimulus pulses applied to each of the stimulating microelectrodes were averaged to obtain an averaged evoked response (AER). For each AER, the amplitude of the first and second component was measured after the averaged response is filtered through a low-pass filter with a bandpass of 250 Hz to 2.5 kHz. The amplitude of the early and second components is measured from the peak of the positivity on the leading edge to the trough of the subsequent negativity (RESULTS, Figure 2). This is repeated for a range of stimulus amplitudes. The response growth function (recruitment curve), which represents the recruitment of the excitable neural elements surrounding the microelectrode, is then generated by plotting the amplitude of the first or second component of each of several AERs against the amplitude of the stimulus pulse that evoked the responses.

The conventional (non-embedded) recruitment curves were generated before and immediately after the sessions of prolonged stimulation. The stimulus frequency was 50 Hz, which is much lower than during the 7-hour test session. In addition, a limited number of "embedded" recruitment curves were acquired during the last 45 minutes of some of the 7-hour sessions of stimulation at 250 Hz. This procedure, which requires approximately 45 minutes per microelectrode, was described in detail in QPR #5.

The conventional (non-embedded) recruitment curves allow detection of depression of neuronal excitability that persists after the termination of the high-rate stimulation with the artificial voice signal. If it is severe, this type of depression may persist for many days. Changes in the non-embedded recruitment curves identify stimulation protocols that place significant stress on the neurons of the lower auditory system. The embedded recruitment curves, in contrast, allows us to determine how the regimen of prolonged stimulation affects the way the neurons respond to the actual artificial voice signal, and to detect short-acting neuronal refractory phenomena

(analogous to forward masking) that would not be apparent in the non-embedded responses. The non-embedded and embedded responses, and the histologic evaluation of the implant sites, together provide a picture of the safety and efficacy of the stimulation regimen.

Within 15 minutes after the end of the last day of stimulation, the cats were deeply anesthetized with pentobarbital and perfused through the aorta with ½ strength Karnovsky's fixative (2.5% glutaraldehyde, 2% paraformaldehyde and 0.1M sodium cacodylate buffer). The cochlear nucleus and adjacent portion of the brainstem were resected, embedded in paraffin, sectioned serially in the frontal plane (approximately parallel to the shafts of the stimulating microelectrodes) at a thickness of 8 μm, and stained with Cresol Violet (Nissl stain) or with hematoxylin and eosin.

RESULTS

Conditioning study in Cat CN-133.

Prolonged microstimulation in the feline ventral cochlear nucleus at high pulsing rates (250 Hz) and at moderate pulse amplitudes, induces a persistent depression of neuronal excitability (SIDNE). This is manifested first as shift in the threshold, and if more severe, in the slope (growth) of the non-embedded recruitment curve of the averaged evoked response (AER) recorded in the inferior colliculus, while stimulating in the cochlear nucleus. Also, during prolonged stimulation at 250 Hz using a (controlled-current) pulse train whose amplitude is modulated according to a realistic acoustic environment (e.g, the artificial voice signal), the embedded recruitment curve becomes shifted to the right of the non-embedded curve. This indicates the occurrence of short-acting neuronal refractory phenomena which may interfere with the performance of the clinical device, by accentuating the "dead-band" at the low end of the range of stimulus amplitudes. We wished to determine if it is possible to reduce the SIDNE and/or the short-acting refractory phenomena, by beginning the stimulation regimen at a low stimulus frequency (100 Hz) and slowly increasing the frequency over a span of many days. The range of stimulus amplitude was the same throughout the regimen, so that the effective spatial spread of the stimulus current is constant, and all of the involved

neurons will be stimulated throughout the regimen. However, that level of stimulation-related stress will be increased gradually as the stimulus frequency is increased. In a previous animal (CN129, QPR #2), the stimulus frequency was increased from 100 Hz to 250 Hz over a span of 15 days. This protocol did not reduce the severity of the SIDNE produced by the prolonged stimulation at 250 Hz. Therefore, in Cat CN133, the stimulus frequency was increased more gradually, over a span of 30 days.

Prior to the start of the conditioning regimen and 56 days after implantation of the electrodes, we conducted a short (2-day) "baseline" study to determine the severity of the SIDNE and the severity of the short-acting refractory phenomena, in the absence of any prior conditioning. Microelectrodes #1, #2 and #3 were pulsed at 250 Hz per electrode in the interleaved mode for 7 hours per day. The stimulus pulse duration was 40 μsec/ph. The stimulus pulse amplitude was modulated across the range of 14-48 μA according to the logarithmically- compressed artificial voice signal with a 50% duty cycle. Figure 2 shows the AER evoked from Microelectrode #1 and recorded in the right inferior colliculus. There is a large early response (presumably evoked directly) and a large second response which probably is evoked transsynaptically. Figure 3 shows the non-embedded and embedded recruitment of the early component of the AER. The effect of the 7 hours of stimulation was quite typical; by the end of the first 7 hours of stimulation, the non-embedded curve had moved to the right. The shift was near the response threshold, indicating persisting depression of the excitability of the neurons close to the microelectrode. The slope of the response above threshold was relatively unaffected. Also, the embedded response curve had shifted to the right of the non-embedded response, revealing some short-acting refractory phenomena, especially near the response threshold. The obvious remedy for this occurrence, (remapping upwards the pulse amplitude that correspond to acoustic silence) is ineffective, since the response threshold promptly increases further. The conditioning regimen is another possible strategy for preserving the full range of the response during high-rate stimulation.

The conditioning regimen was initiated 14 days after the baseline study described above, after the SIDNE had disappeared. Except for the pulsing rate, the

stimulus conditions were identical to those used in the baseline study. The stimulus pulse frequency was 100 Hz per electrode for the first 10 days, 150 Hz for the second 10 days, 200 Hz for the third 10 days, and then 3 days at 250 Hz. On the 34th day, only electrode #1 was pulsed for 7 hours, at 250 Hz, as part of a special experiment that is described below. Figure 4 shows the non-embedded recruitment of the early component of the AER evoked from Microelectrode #1 during the first 19 days of the regimen. The curves lie very close together and very close to the prestimulus (control) non-embedded curve, indicating very little SIDNE. There was a very small increase in the response threshold when the pulse rate was 150Hz . Figure 5 shows the non-embedded and embedded recruitment curves of the first component of the AER evoked from Microelectrode #1. This data was acquired at the end of the 14th day of pulsing and the fourth day of pulsing at 150 Hz. The embedded and non-embedded responses are very similar and both lie very close to the prestimulus (control) non-embedded curve. Thus, there very little short-acting refractory phenomena.

As the pulsing rate was increased to 250 Hz, SIDNE became more pronounced, and the non-embedded recruitment curve shifted to the right of the control curve (Figure 6A, from microelectrode #1). Also, the embedded recruitment curve diverged from the non-embedded curve, revealing more short-acting refractory phenomena. Figure 6B shows similar data, also from microelectrode #1, which was acquired on the 34th day, with only electrode 1 pulsed at 250 Hz.

Did the conditioning regimen reduce SIDNE or the short-acting refractory phenomena when the pulsing rate finally reached 250 Hz? Figure 7A shows the non-embedded recruitment of the first component of the AER evoked from Microelectrode #1 and acquired after the second day of the baseline study (which was not preceded by a conditioning regimen). The second curve was acquired at the end of the conditioning regimen and after the third day of stimulation at 250 Hz. The thresholds of the responses is virtually identical, but the slope of the AER was slightly steeper at the end of the conditioning regimen. Thus, the conditioning regimen did not protect the neurons very close to the microelectrode from SIDNE but may have slightly reduced an inhibitory effect in the neurons further from the electrode. Even here, we must be cautious, since

the curves were generated from data acquired 48 days apart, and the slope of the recruitment curves may change slightly from month to month, even when the response thresholds are stable. Figure 7B shows the recruitment curve of the embedded response, acquired on the last day of the baseline study, and on the last day of the conditioning regimens. Here also, the response thresholds are virtually identical, and we conclude that the conditioning regimen did not prevent the occurrence of the dead-band at the low end of the amplitude range. It is uncertain how a dead-band in the low end of the range of neurons responses would affect the performance of a clinical device. With logarithmic compression of the acoustic signal, most of the speech is mapped to pulse amplitudes in the upper half of the amplitude range, as illustrated in Figure 1. Degraded performance might occur if the speech processor does not contain a fast automatic gain control, permitting the pulse amplitudes representing quiet speech would tend to fall in the dead-band (even with the logarithmic compression.)

Although the conditioning regimen did not prevent the occurrence of an acoustic dead-band when the pulse frequency is high, a comparison of Figures 5 and 6B does suggest another strategy. In this cat, the 3 pulsed microelectrodes were spaced 400 μm apart. When all 3 microelectrodes were pulsed in the interleaved mode at 150Hz for 7 hours, the stimulation induced very little shift in the recruitments curves. However, when only a single microelectrode (#1) was pulsed for 7 hours at 250 Hz (Figure 6B) the embedded and non-embedded recruitment curves still became shifted to the right of the pre-stimulus, non-embedded (control) curve. Thus, it may be advantageous to distribute the stimulation over 2 or 3 electrode sites separated by a few hundred μm, and to pulse each site at a lower rate. This strategy may reduce the spatial resolution of the microstimulation system, but in the ventral cochlear nucleus it may be possible to distribute the stimulation across several electrode sites located in the same tonotopic lamina, and thus, not seriously degrade resolution across the tonotopic gradient. Of course, this would require a microelectrode array with many more independent stimulation sites.

Effect of prolonged, high-amplitude stimulation

Thirty-seven days after the end of the conditioning regimen, cat CN133 was used in another study in which the electrodes were pulsed at high amplitude on 18 successive days. This was part of a project to determine the maximum safe stimulus pulse amplitude that could be used when the pulse amplitude is short (40 μsec/ph) and the current density at the electrode tissue interface is correspondingly high. The objective of this particular part of the study was to determine if the use of microelectrodes with larger geometric surface areas, and therefore, lower current densities, would prevent some of the suspicious histologic and physiologic effects that we have previously observed when the electrode current density is high (e.g., Cat CN125 and CN126, as described in QPR #2).

In cat CN130 and in the previous animals, the electrode surface area was approximately 1,000 μm^2 ±150 μm^2, while cat CN133 is the first of 3 animals in which the geometric area was 2,000 ±300 μm^2. The 11-day stimulation regimen for CN130 was begun 279 days after implantation of the array. Three of the 4 microelectrodes (#1, #2, #4) in the PVCN were pulsed for 7 hours per day, at 250 Hz. Microelectrode #3 was not pulsed, but was permanently shorted to the platinum ground, as part of a special test described in the last section of this report. The amplitude of the control current pulses was modulated according to the logarithmically-compressed artificial voice signal with a 50% duty cycle. The pulse amplitude was modulated over the range of 14-63 μA (63 μA is the maximum amplitude that can be generated by our stimulation backpack when it is in the standard microstimulation condition). The stimulus pulse duration was 40 μsec/ph. In Cat CN130, the amplitude of the early component of the AER was very small, so the physiologic measurements were obtained from the second component, which presumably is evoked transsynaptically. Figure 8A shows the non-embedded recruitment of the second component of the AER evoked from Microelectrode #1. After the first 7 hours of stimulation, the non-embedded recruitment of the response from microelectrode #1 was shifted to the right of the control curve. By the end of the second day of stimulation, the curve had shifted slightly further, at which point it stabilized for the reminder of the 11-day regimen. Figure 8B shows the non-

embedded responses evoked from microelectrode #2. The curve acquired at the end of the 11th day is shifted somewhat to the right of those acquired at the end of the first 6 days, indicating some worsening of the SIDNE throughout the 11-day regimen.

Immediately after the 11th day of stimulation, the cat was sacrificed for histologic evaluation of the electrode sites. Figures 9A, B, C, D show the sites of the tips of microelectrodes 1, 2, 3 and 4 in the PVCN. These micrographs are from histologic sections cut in the frontal plane, and slightly oblique to the dorsoventrally-directed tracks (shafts) of the microelectrodes. Dorsal is at the top of the photos. The gliotic sheath around the tip (T) of pulsed microelectrode #1 (Figure 9A) is surrounded by normal-appearing neuropil, and the neurons (N) close to the tip appear to be normal. However, there does appear to be some proliferation and/or infiltration of glial cells into the sheath, and many darkly-stained, irregularly-shaped glial cells (probably astrocytes) are intercalated into the fibrotic sheath surrounding the tip, and the sheath itself appears to be somewhat thicker than usual. This phenomena is even more evident around the tip of (pulsed) microelectrode #2 (Figure 9B), and may be the histologic basis of the progressive shift in its recruitment curves, as noted above. Some lymphocytes had infiltrated into the gliotic sheath and are interspersed with the glial cells. Similarly, the tip of pulsed microelectrode #4 (Figure 9C) is surrounded by many glial cells. There are notably fewer glial cells intercalated into the sheath around the tip of unpulsed Microelectrode #3 (Figure 9D) . In summary, there was no histologic evidence that the high amplitude electrical stimulation injured the nearby neurons or neuropil, but there were some indications that the stimulation had induced some reactive gliosis around the electrode tips.

In cat CN133, the electrode's geometric surface areas were larger (2,000 ± 200 μm^2). An 18-day stimulation regimen was initiated 151 days after implantation of the days and 37 days after the end of the 33-day conditioning study. We assume that any effect of the conditioning study would have dissipated by this time. The stimulus parameters used in the 18-day regimen were identical to those used in cat CN130 as described above. Microelectrodes 1, 2 and 4 were pulsed using the same parameters as in cat CN130.

Figure 10A shows the non-embedded recruitment of the first component of the AER evoked from microelectrode #1. Figure 10B shows the recruitment of the second component . Figure 11A and 11B show the non-embedded recruitment of the first and second component evoked from microelectrode #2. All show a moderate amount of SIDNE at the end of the first day of stimulation, but the recruitments curves did not shift further during the next 17 days of the regimen.

The cat was sacrificed immediately after the 18th day of stimulation. Figure 12A shows the site of the tip of pulsed microelectrode #1. Neurons (N) and neuropil surrounding the site of the microelectrode tip (T) appear to be normal and healthy. The gliotic sheath surrounding the tip is thin and appeared very similar to the sheath surrounding the unpulsed microelectrode #3 (Figure 12C). Figure 12B shows the site of the tip of (pulsed) microelectrode #2. Here also, the neurons and neuropil surrounding and subjacent to the tip site appear normal and healthy, and there is no indication of active gliosis. The site of the tip of microelectrode #4 was not found, due to problems with the histologic processing.

The results from Cat CN133 indicate that the cochlear nucleus can tolerate prolonged stimulation, using short-duration, high-amplitude current pulses which are amplitude-modulated according to a signal designed to simulate a fairly noisy acoustic environment. In Cat CN133, the recruitment curves of the AER were very stable over the last 17 days of the 18-day stimulation. The stimulation did induce a modest increase in the threshold of the AER, but the threshold did not increase further after the first day of stimulation. In cat CN133, the microelectrode's geometric surface areas were larger than in previous animals that had been subjected to prolonged stimulation in protocols in which the stimulus amplitude reached 60-63 μA (Cats CN125, CN126, described in qpr#2 and CN130 described in the present report). In these 3 animals, the microelectrodes' geometric surface area was approximately 1,000 μm^2. In no case was there histologic evidence of neuronal injury. However, in all 3 of these animals, the prolonged high-amplitude stimulation produced some histologic and/or physiologic manifestations that were a bit disconcerting. In all three cats, the recruitments curves of the evoked responses from at least some of the microelectrodes continued to shift

slightly to the right throughout the prolonged stimulation regimens (e.g. Figure 8B). In cats CN125 and CN130, there was some evidence of active gliosis around the tip of the pulsed microelectrodes (Figure 9). This type of tissue reaction is difficult to quantify, since the thickness of the gliotic sheath near the electrode tips is somewhat variable, and even the sheath around the tips of unpulsed microelectrodes frequently is infiltrated with at least a few glial cells. Also, there often are small gliotic scars adjacent to one side of the tip sites, which are probably related to mechanical trauma during or subsequent to implantation of the microelectrodes (e.g, Figure 9D). However, the capsules around these pulsed tips sites do appear to be distinctly darker than normal, and they contrast strongly against the surrounding neuropil, a feature that is difficult to capture in the black-and white photomicrographs. If gliosis is indeed accelerated near the tips of the pulsed microelectrodes, it may be related to the higher current density used in conjunction with the short-duration current pulses. In these animals, the maximum charge density and charge per phase (2.5 nC/ph) was less than in numerous regimens of prolonged stimulation using longer duration (150 μsec/ph) pulses, in which the charge per phase reached 3 nC. In those animals, the recruitment curves of the AERs usually were very stable after the first day of stimulation and there was no evidence of active gliosis at the electrode tips (We did observe active gliosis at sites randomly distributed along the electrode shafts. This type of "toxic" gliosis seems to be related to micro-foci of contaminants on the electrode shafts. It has a loosely-consolidated appearance, and is distincly different from the compact gliotic sheaths and small scars surrounding and adjacent to the tip sites. We are addressing the issue of the sporadic "toxic" gliosis in all three of our microstimulation contracts).

In cat CN133, in which the high-amplitude stimulation did no appear to provoke any tissue reaction (Figure 12) the electrode's surface areas were larger than in cats CN125 , CN126, and CN130, and therefore, the current density was lower. However, we must be cautious about drawing conclusions from a single animal. Also, The interpretation of the data from Cat CN133 is complicated somewhat by the fact that the animal was used in the baseline protocol preceding the conditioning regimen, and in the 33-day conditioning regimen which ended 37 days prior to initiation of the final 18-day

high-amplitude stimulation protocol. Finally, even if the stimulation does promote some gliosis at the electrode tip, the functional implications of such a tissue response is as yet undetermined. If the stimulation does promote gliosis, and if this results in a thickening of the sheath around the electrode tips, then the excitable neural elements would be pushed away from the electrode tip, and we would expect an increase in the threshold of the evoked response, as depicted in Figure 8B. We have implanted 2 additional animals with microelectrode that have surface areas of approximately 2000 μm^2, and these animals will be stimulated during the next quarter of the contract. We also will stain the tissue around the tips of some of these electrodes for GFAP, a protein that is expressed in reactive glia cells. Meanwhile, we have not observed any evidence of reactive gliosis at the electrode tip sites, or a progressive shift in the recruitment curves of the evoked response during prolonged stimulations, when the stimulus amplitude of the 40 μs pulses was not allowed to exceed 48 μA (QPR #2). In those cats, the geometric surface areas of the microelectrodes was approximately 1000 μm^2. At present, we recommend 48 μA as the maximum amplitude of the 40 μs stimulus pulses, under the conditions delimited in this report.

Electrode shorting experiment.

The first clinical trials of the cochlear nucleus microstimulation array will use the Cochlear Corporation CI24M sound processor and stimulator system. This device was designed for cochlear implants. There are no isolation capacitors in the output channels, and in the interval between the controlled-current stimulus pulses, the output channels are connected to the ground electrode. Since the intranuclear microstimulation array will be integrated with an array of platinum macro electrodes that will be inserted into the lateral recess of the patient's 4th ventricle, the ground electrode also should be of platinum. When small (or micro) electrodes are connected to a large ground electrode, the potential of the small electrode is pulled to the equilibrium potential of the large ground. Thus, if the ground and working electrodes are of different materials, there is the possibility that a small DC current would pass between them, and through the tissue. The equilibrium potential of activated iridium is slightly

positive of the equilibrium potential of platinum when both are immersed in physiological saline, so if the ground electrode were to be fabricated from iridium in order to accommodate the iridium microelectrodes, then the potential of the platinum macro-electrodes comprising the lateral recess array would be pulled positive of their normal equilibrium potentials, and this might increase their rate of dissolution (Cogan, Personal Communication). We therefore propose to fabricate the ground electrode from platinum (as in the present ABI device) and to determine if there are untoward consequences of permanently shorting an activated iridium working electrode to the platinum ground. This configuration will pull the potential of the iridium electrodes approximately 50 mV negative of their normal equilibrium potential.

In cat CN130, microelectrode #3 was intentionally connected directly and permanently to the platinum ground electrode, for a total of 61 days. Figure 13 shows the non-embedded recruitment of the second component of the AER recorded in the inferior colliculus before microelectrode #3 was shorted to ground, and a second curve acquired 61 days later, just before the cat was sacrificed. The threshold and slope of the response is almost unchanged (in fact, the threshold is very slightly lower after 61 days). This indicates that shorting the iridium electrode to the platinum ground did not adversely effect the electrical excitability of the neurons very close to the microelectrode tip. The cat was sacrificed immediately after the 61st day of the study. Figure 9D shows a histological section through the site of the tip of Microelectrode #3. The neurons and neuropil appear to be quite normal, and the gliotic capsule surrounding the tip is not unusually thickened. These physiologic and histologic findings indicate that activated iridium microelectrodes can be safely shorted to a platinum ground. It is notable that this arrangement will shift the interpulse potential of the iridium microelectrodes to a value that is slightly negative of their equilibrium potential in physiologic fluid, and this certainly will reduce their charging capacity. (The charge capacity of these electrodes is optimal when they are biased to 300-400 mV positive of their normal equilibrium potential.) This loss of charge capacity is another argument for using microelectrodes with somewhat larger surface areas, for this particular application.

.....

Acknowledgment: We thank Stuart Cogan of EIC Corporation for his consultations on the issue of iridium microelectrodes being shorted permanently to a platinum ground.

The artificial voice signal was specified by Working Party Q.12/XII, The International Telegraphic and Telephony Consultive Convention (CCITT), Geneva, Switz., (January, 1988).

Distribution of stimulus pulse amplitudes derived from Logarithmically-compressed artificial voice signal, shifted and scaled to range from 14 to 63 μA

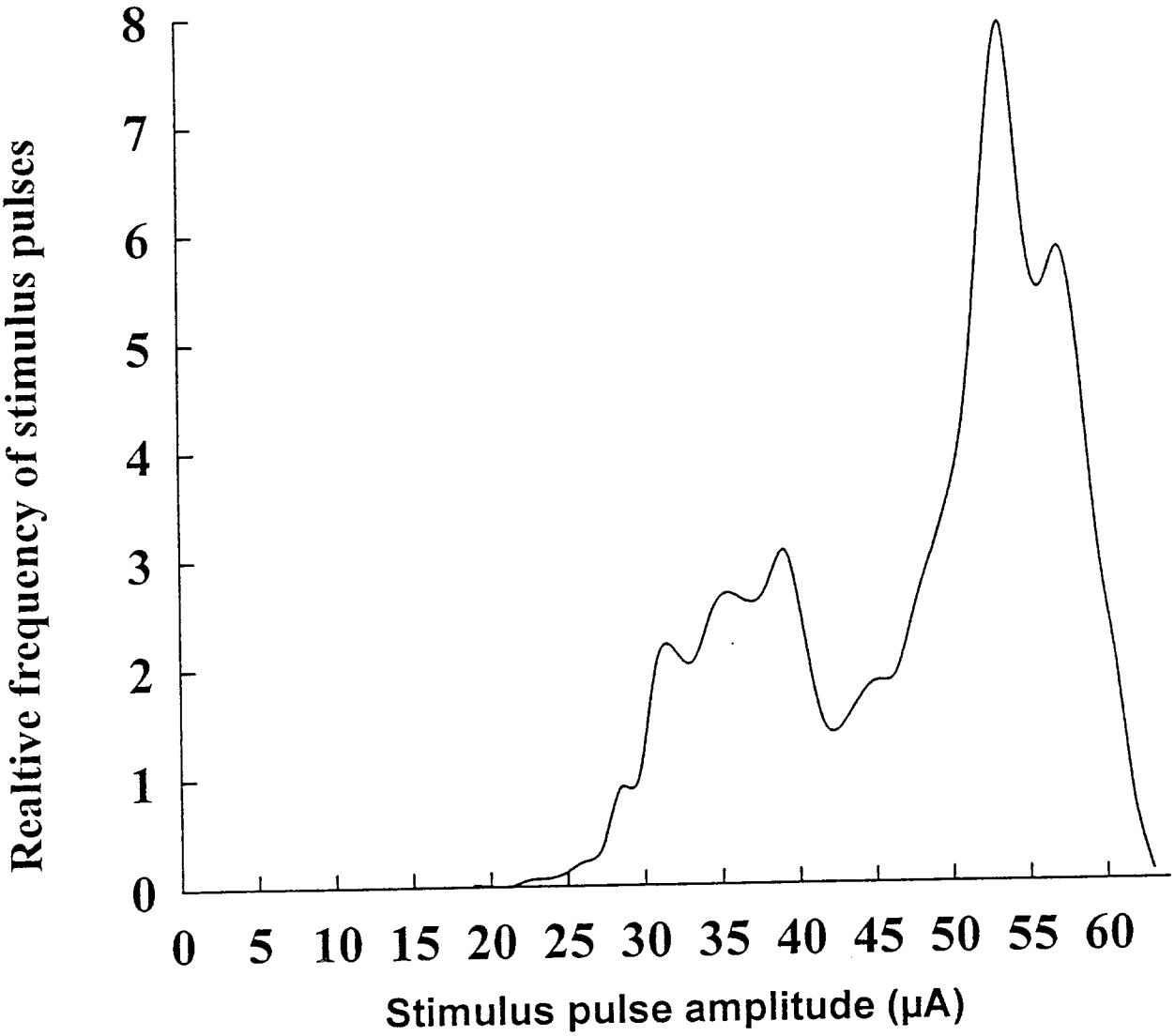

e:\spw\cn\artvoi.spw

Figure 1

cat cn133
Averaged evoked response, by stimulating in PVCN
with 40 μA (40 μs) pulses and recording in the inferior colliculus

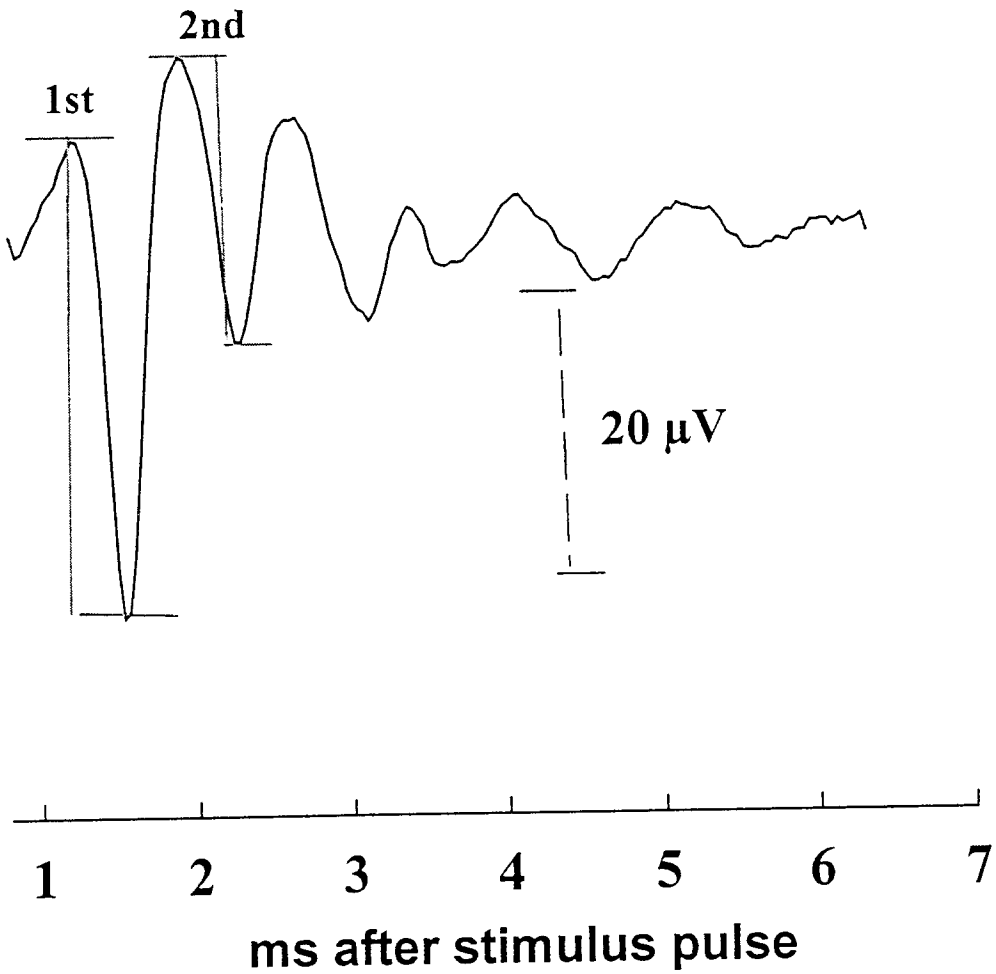

e:/spw/cn/cn133a.spw

Figure 2

cat cn133
Electrodes 1,2,3 pulsed over the range of 14-48 μA, 250 Hz, 7 hrs/day
according to log-compressed artificial voice signal with 50% duty cycle

Non-embedded response evoked from microelectrode #1

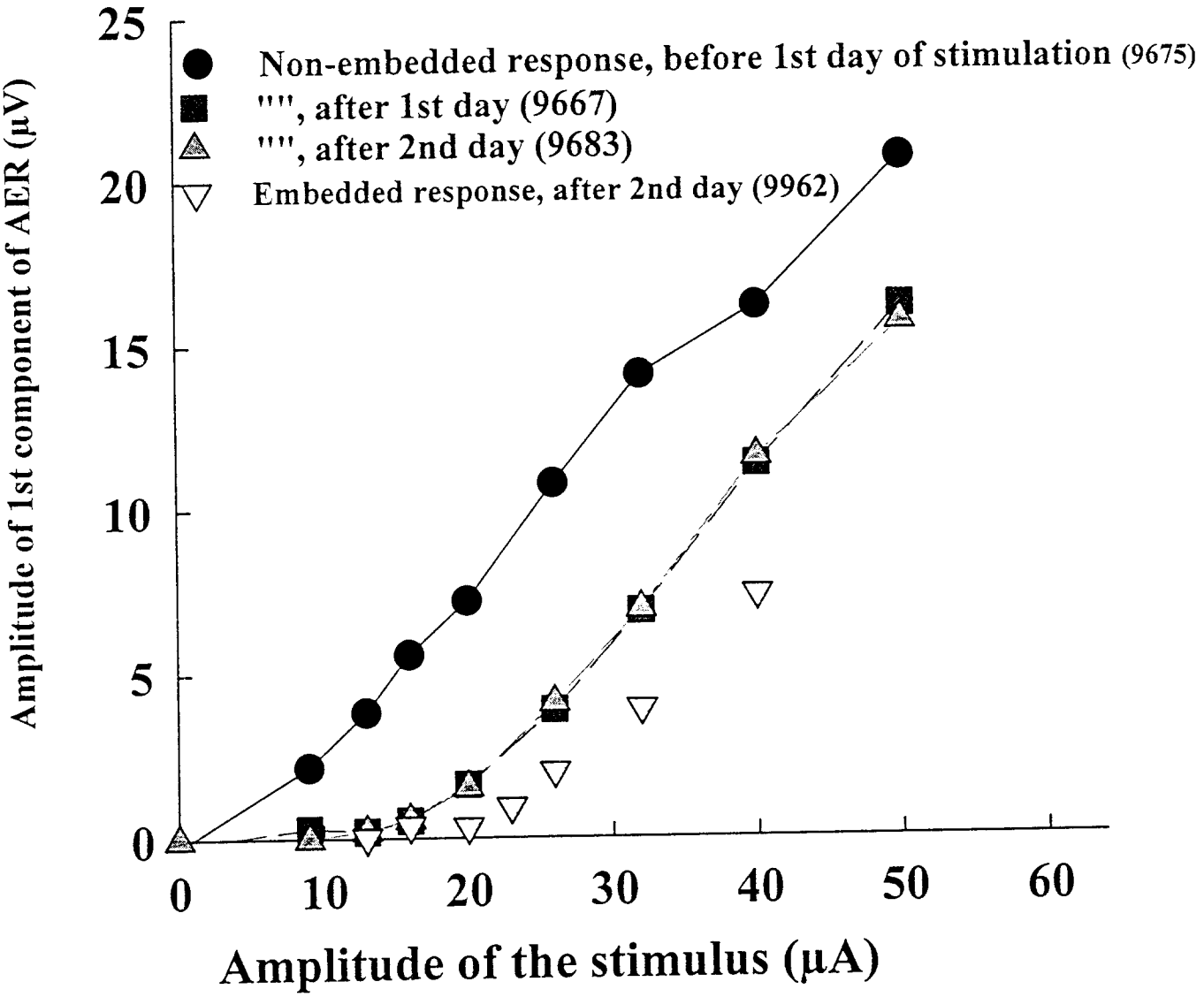

e:/spw/cn/cn133e1m.spw

Figure 3

cat cn133
33-day Conditioning study, using gradually increasing pulse frequency.
Electrodes 1,2,3 pulsed over the range of 14-48 µA, 40 µs/phase, 7 hrs/day
according to log-compressed artificial voice signal, with 50% duty cycle.

Non-embedded responses evoked from microelectrode #1

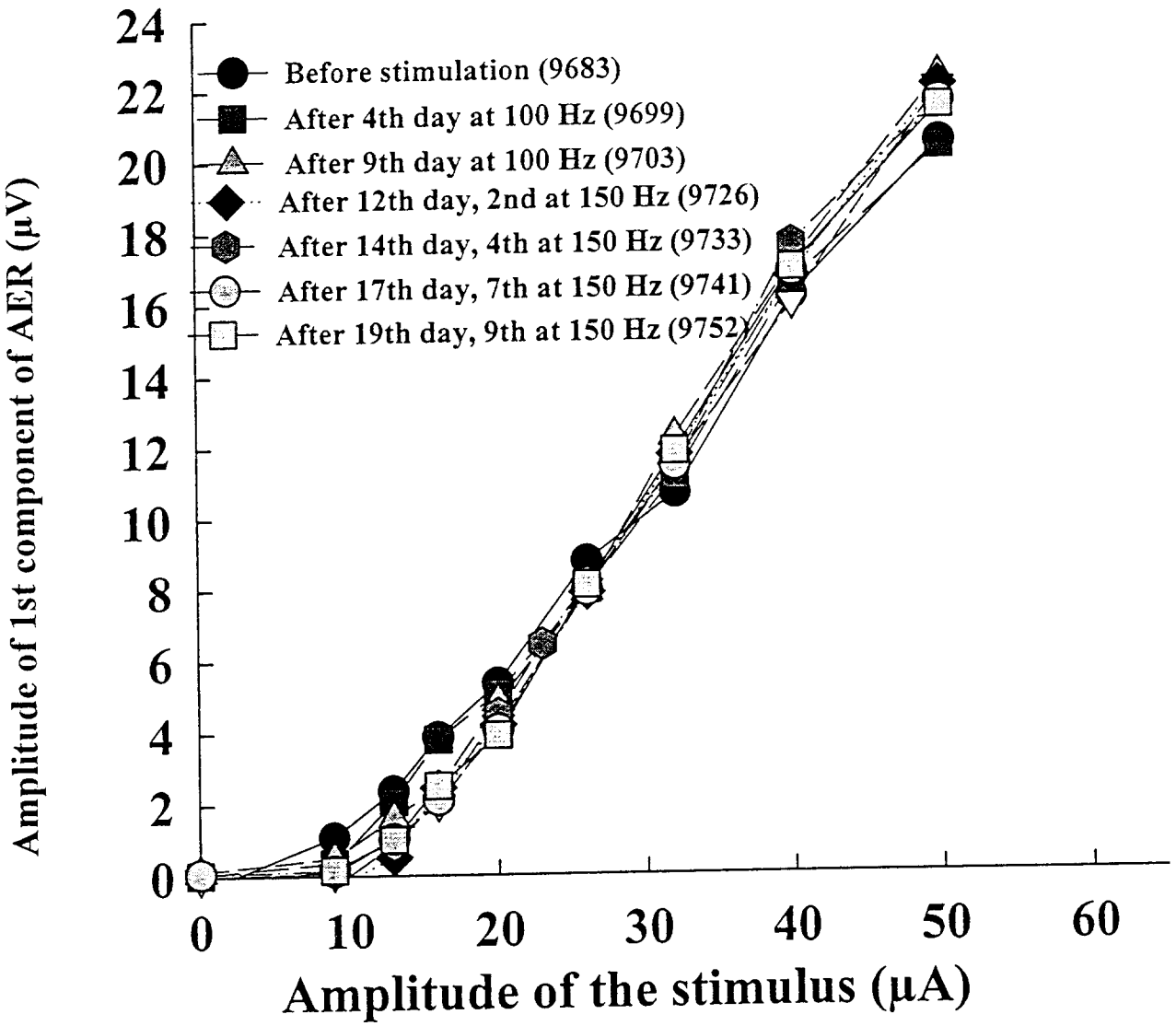

e:/spw/cn/cn133e1r.spw

Figure 4

cat cn133
33-day conditioning study, using gradually increasing pulse frequency
Electrodes 1,2,3 pulsed over the range of 14-48 μA, 40 μs/phase, 7 hrs/day
according to log-compressed artificial voice signal, with 50% duty cycle

Non-embedded & embedded responses evoked from microelectrode #1

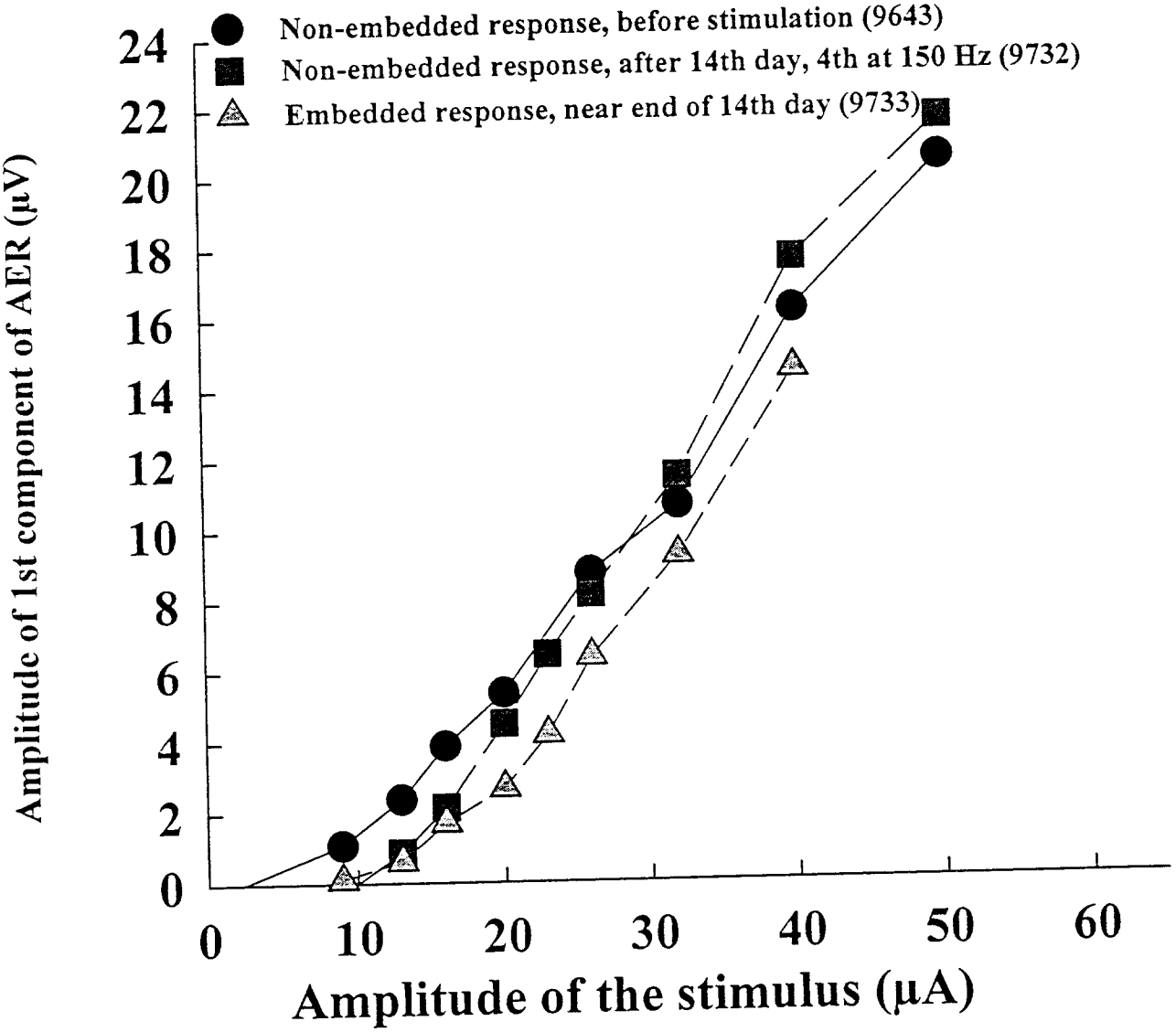

e:/spw/cn/cn133co3.spw

Figure 5

cat cn133
Conditioning study, using gradually increasing pulse frequency
Electrodes 1,2,3 pulsed over the range of 14-48 μA, 250 Hz, 7 hrs/day
according to log-compressed artificial voice signal, with 50% duty cycle.

Non-embedded & embedded responses evoked from microelectrode #1

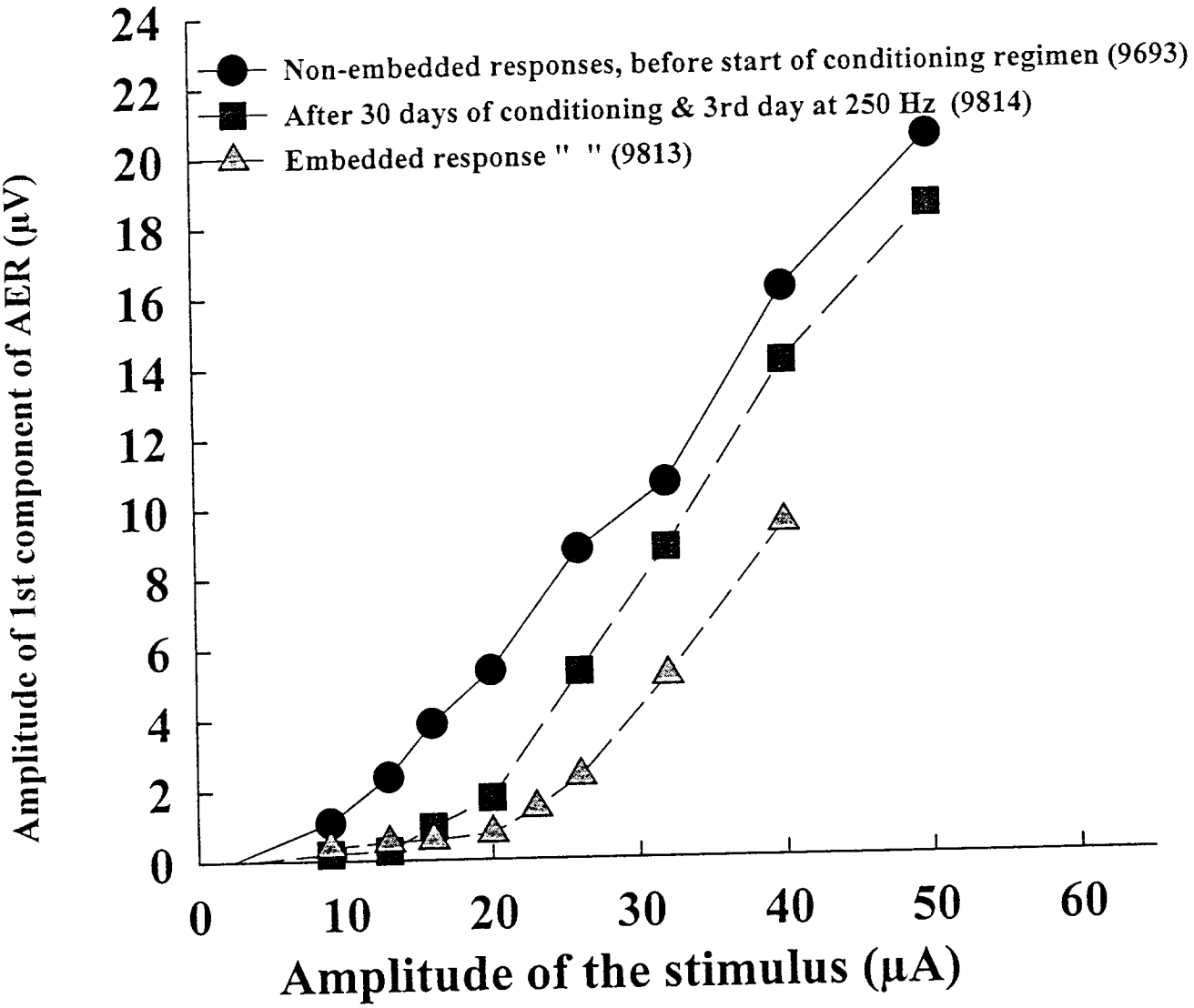

e:/spw/cn/cn133e1z.spw

Figure 6A

cat cn133
Conditioning study, using gradually increasing pulse frequency
Only electrodes 1 was pulsed, over the range of 14-48 µA, 250 Hz, 7 hrs/day
according to log-compressed artificial voice signal, with 50% duty cycle.

Non-embedded & embedded responses evoked from microelectrode #1

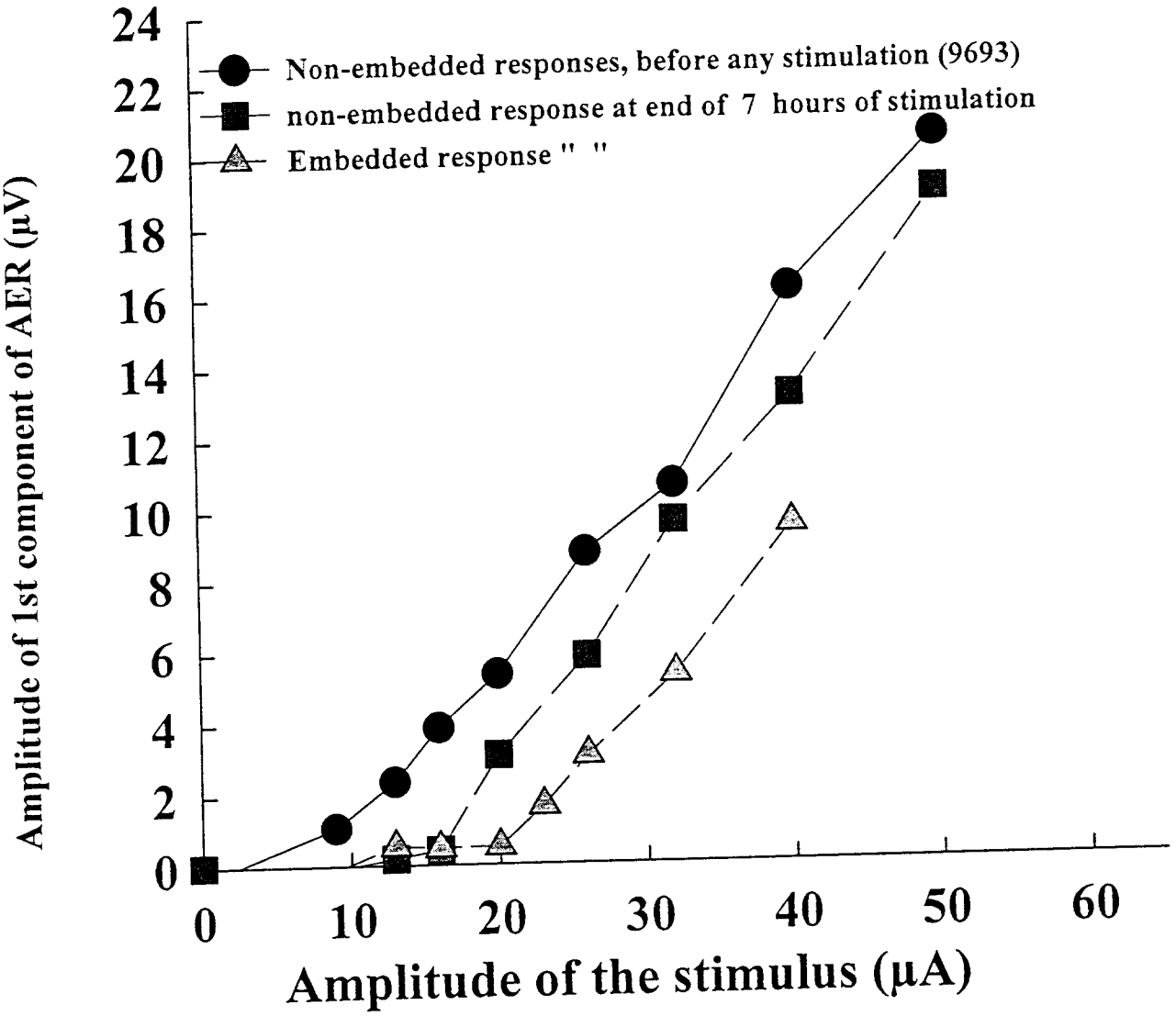

e:/spw/cn/cn133co5.spw

Figure 6B

Comparison of response from electrode 1 after 2-day regimen
not preceded by conditioning, and after 30-day conditioning regimen.
Non-embedded responses evoked from electrode #1
Electrode 1,2,3 pulsed over the range of 14-48 μA for 7 hrs/day,

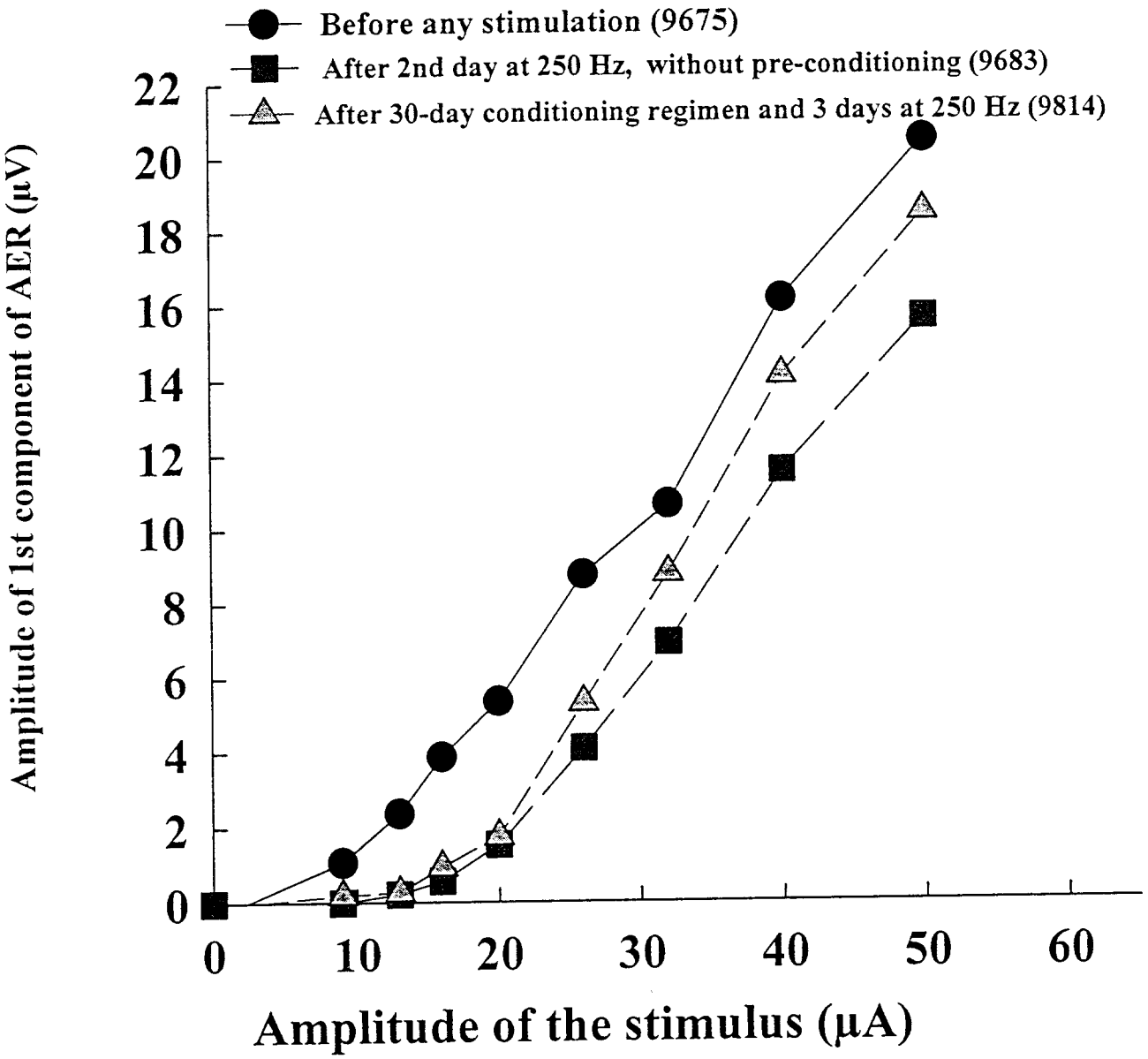

e:\spw\cn\cn133co1.spw

Figure 7A

Comparison of response from electrode 1 after 2-day regimen
not preceded by conditioning, and after 30-day conditioning regimen.
Embedded responses evoked from electrode #1
Electrode 1,2,3 pulsed over the range of 14-48 μA for 7 hrs/day,

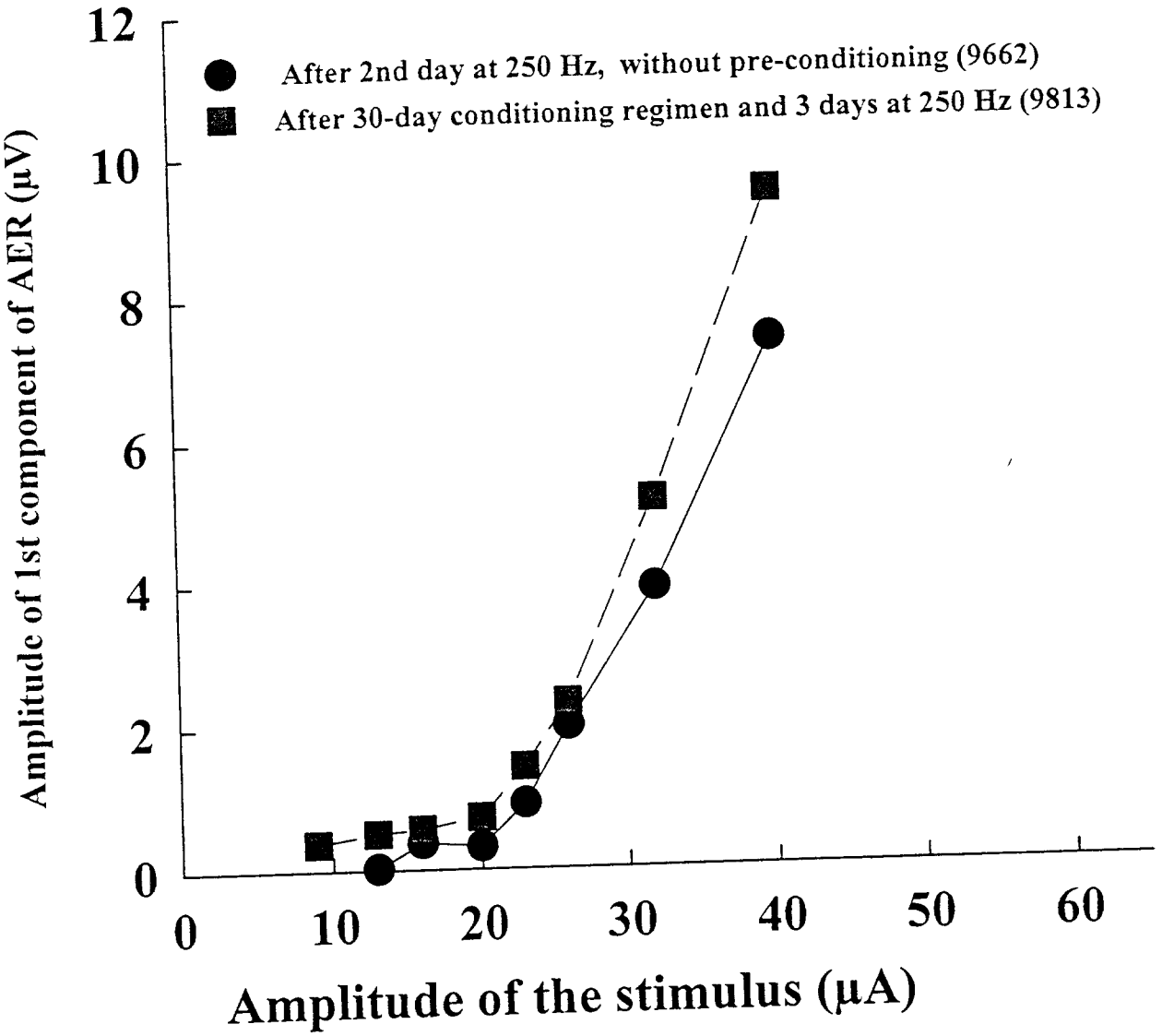

e:\spw\cn\cn133co2.spw

Figure 7B

cat cn130
Electrodes 1,2 ,4 pulsed over the range of 14-63 µA, 40 µs/phase, 250 Hz, 7 hrs/day according to log-compressed artificial voice signal, with 50% duty cycle.

Non-embedded responses evoked from microelectrode #1

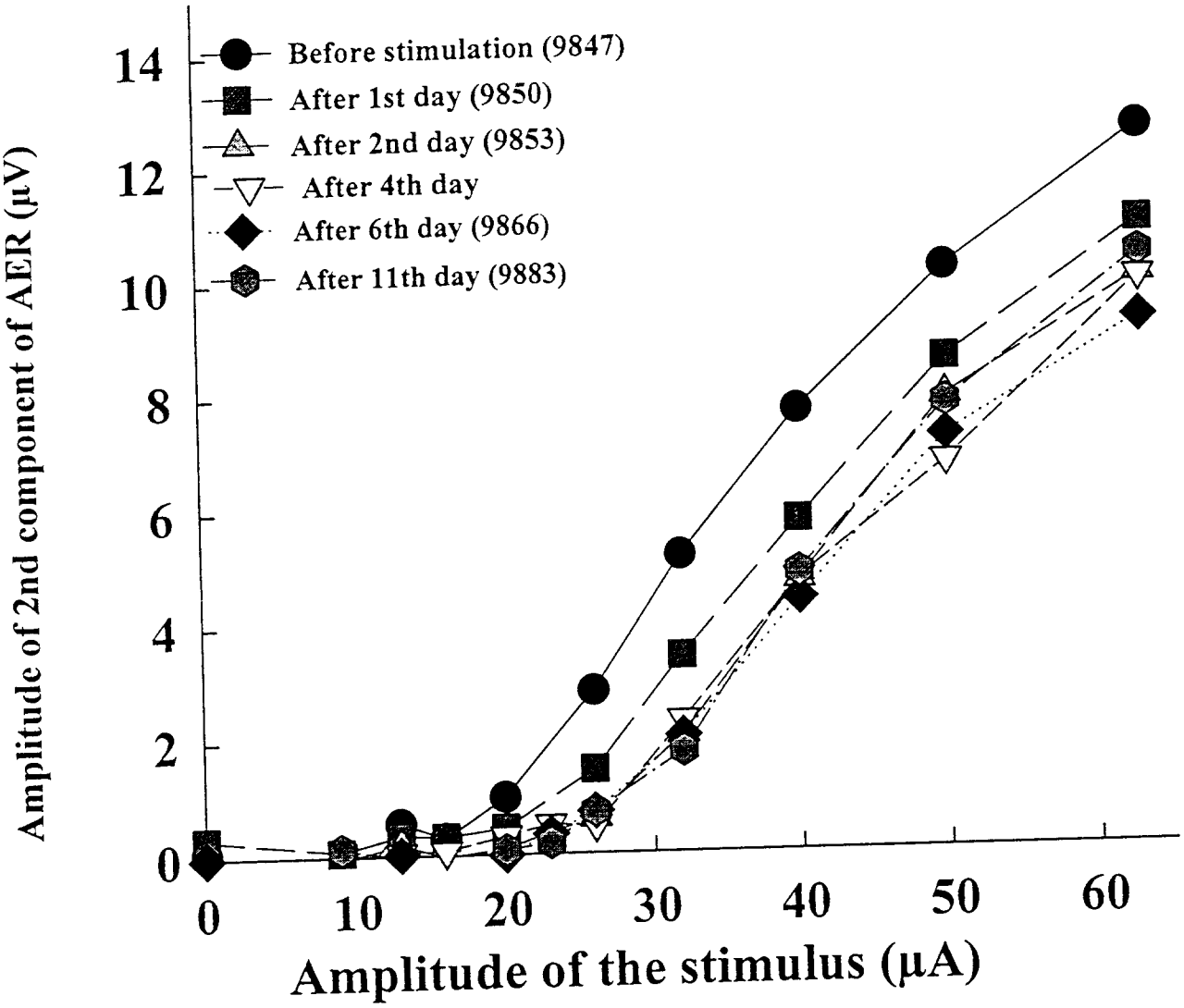

e:/spw/cn/cn130f1.spw

Figure 8A

cat cn130
Electrodes 1,2, 4 pulsed over the range of 14-63 µA, 40 µs/phase, 250 Hz, 7 hrs/day according to log-compressed artificial voice signal, with 50% duty cycle.

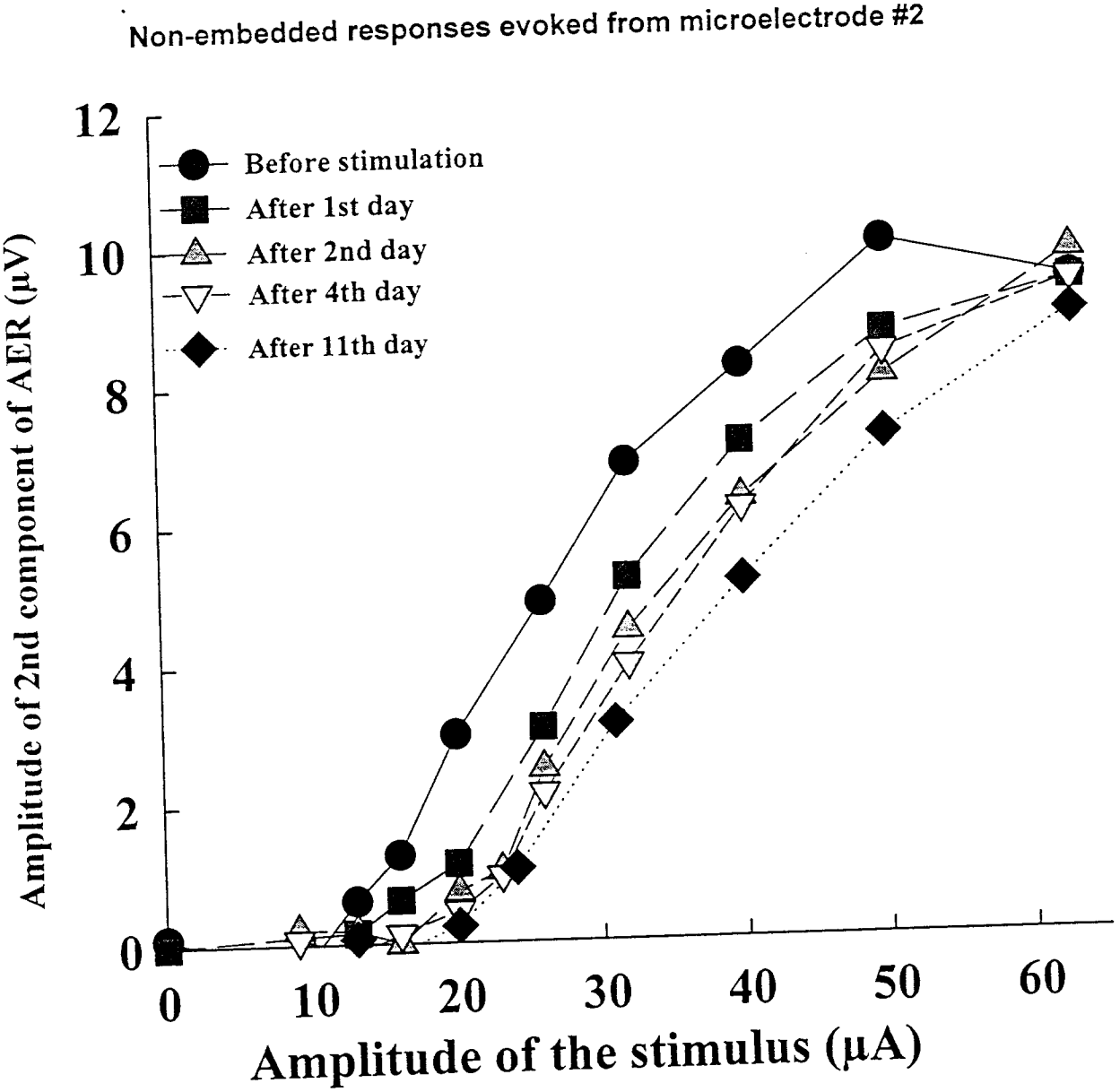

e:/spw/cn/cn130f2.spw

Figure 8B

Figure 9A: cat CN130. Tip of (pulsed) electrode #1. Bar = 100 µm

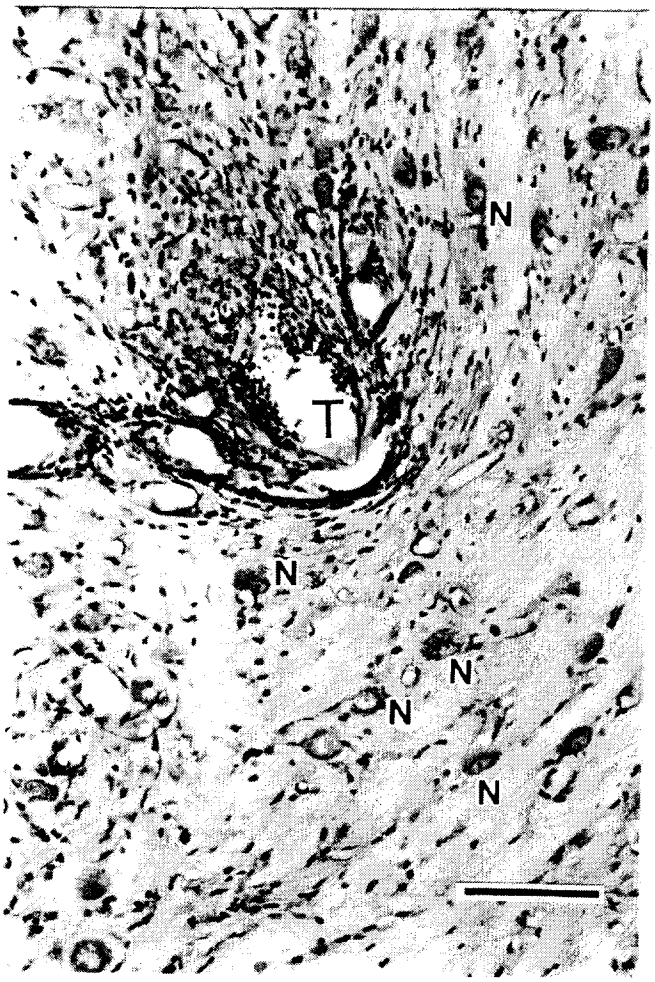

Figure 9B. cat CN130. Tip of (pulsed) electrode #2

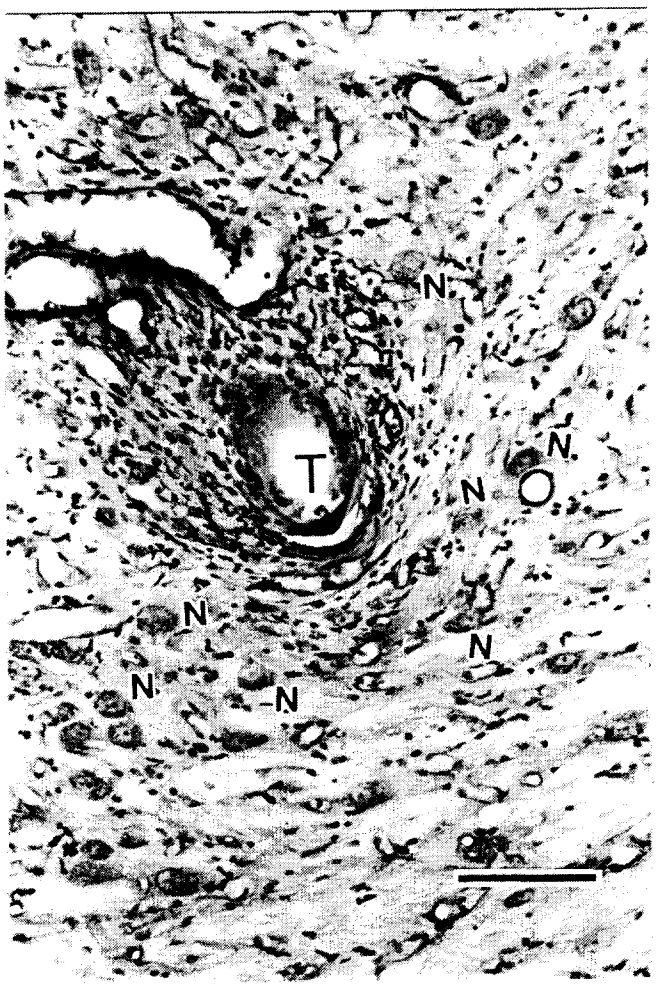

Figure 9C: cat CN130. Tip of (pulsed) electrode #4. Bar = 100 µm

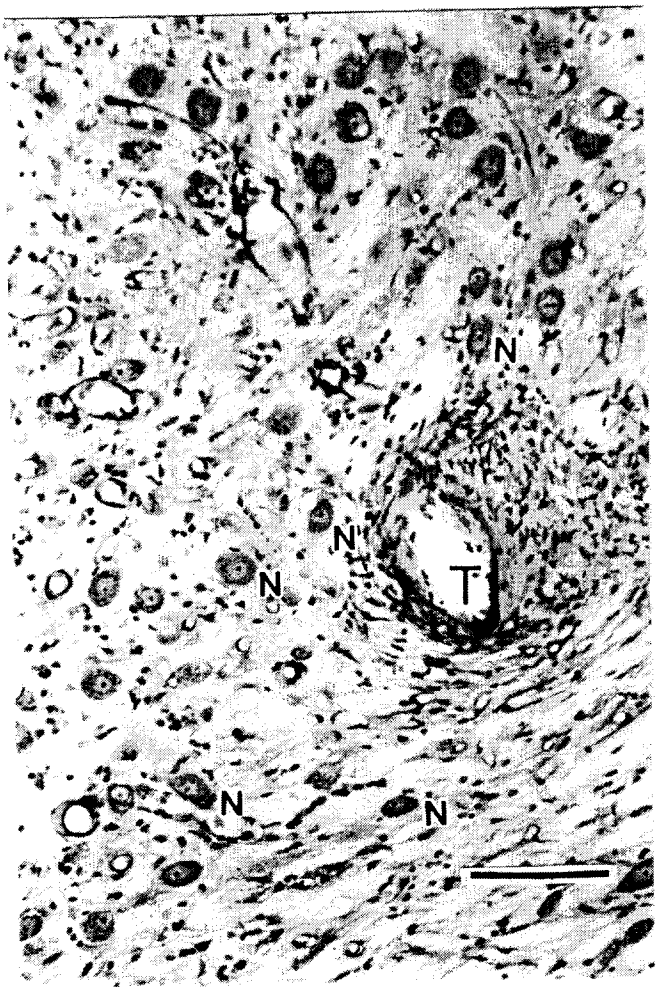

Figure 9D. cat CN130. Tip of (unpulsed) electrode #3

cat cn133
Electrodes 1,2, 4 pulsed over the range of 14-63 μA, 40 μs/phase, 250 Hz, 7 hrs/day according to log-compressed artificial voice signal, with 50% duty cycle.

Non-embedded responses evoked from microelectrode #1

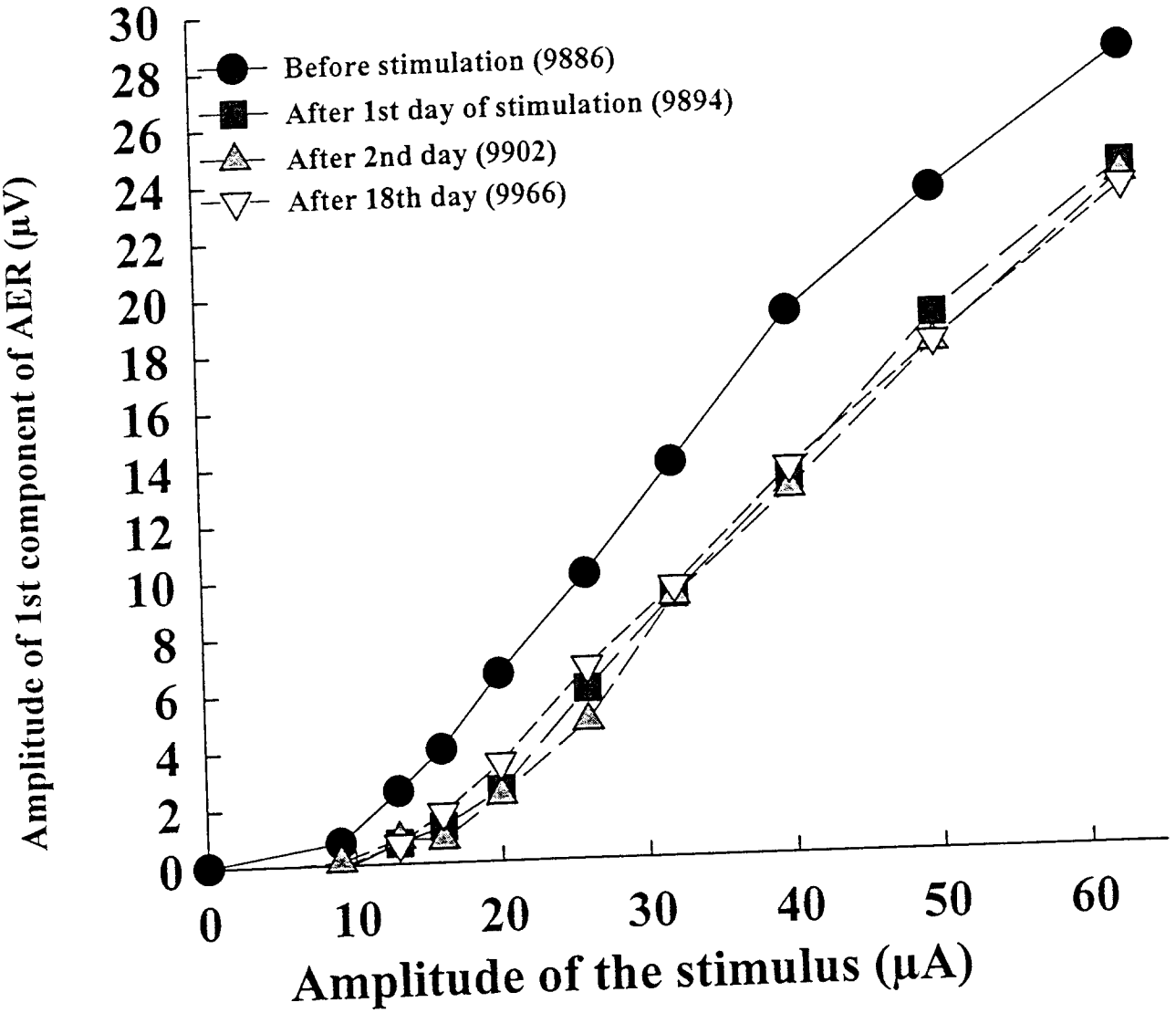

e:/spw/cn/cn133ae1.spw

Figure 10A

cat cn133
Electrodes 1,2,4 pulsed over the range of 14-63 µA, 40 µs/phase, 250 Hz, 7 hrs/day according to log-compressed artificial voice signal, with 50% duty cycle.

Non-embedded responses evoked from microelectrode #1

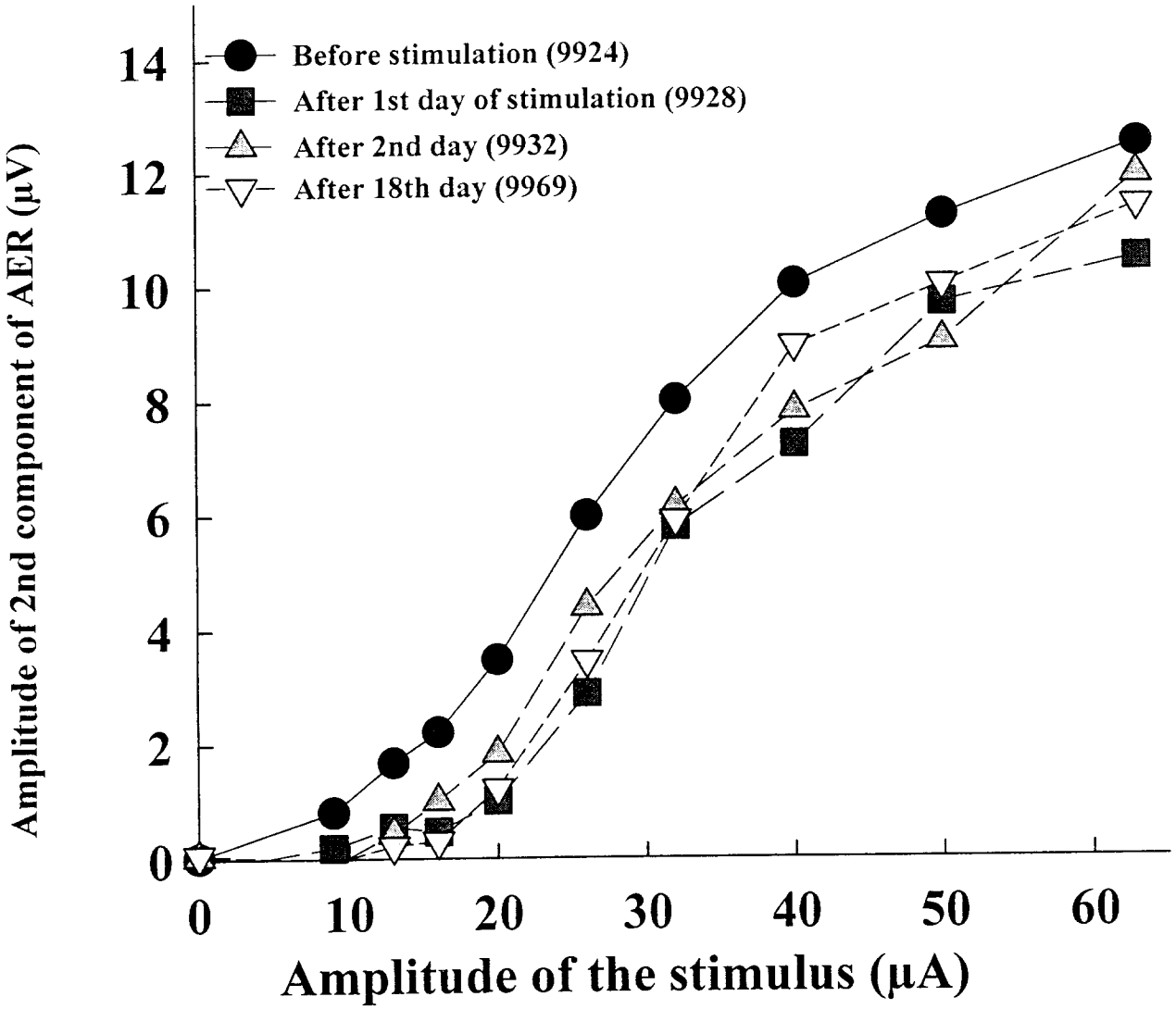

e:/spw/cn/cn133a11.spw

Figure 10B

cat cn133
Electrodes 1,2,4 pulsed over the range of 14-63 μA, 40 μs/phase, 250 Hz, 7 hrs/day according to log-compressed artificial voice signal, with 50% duty cycle.

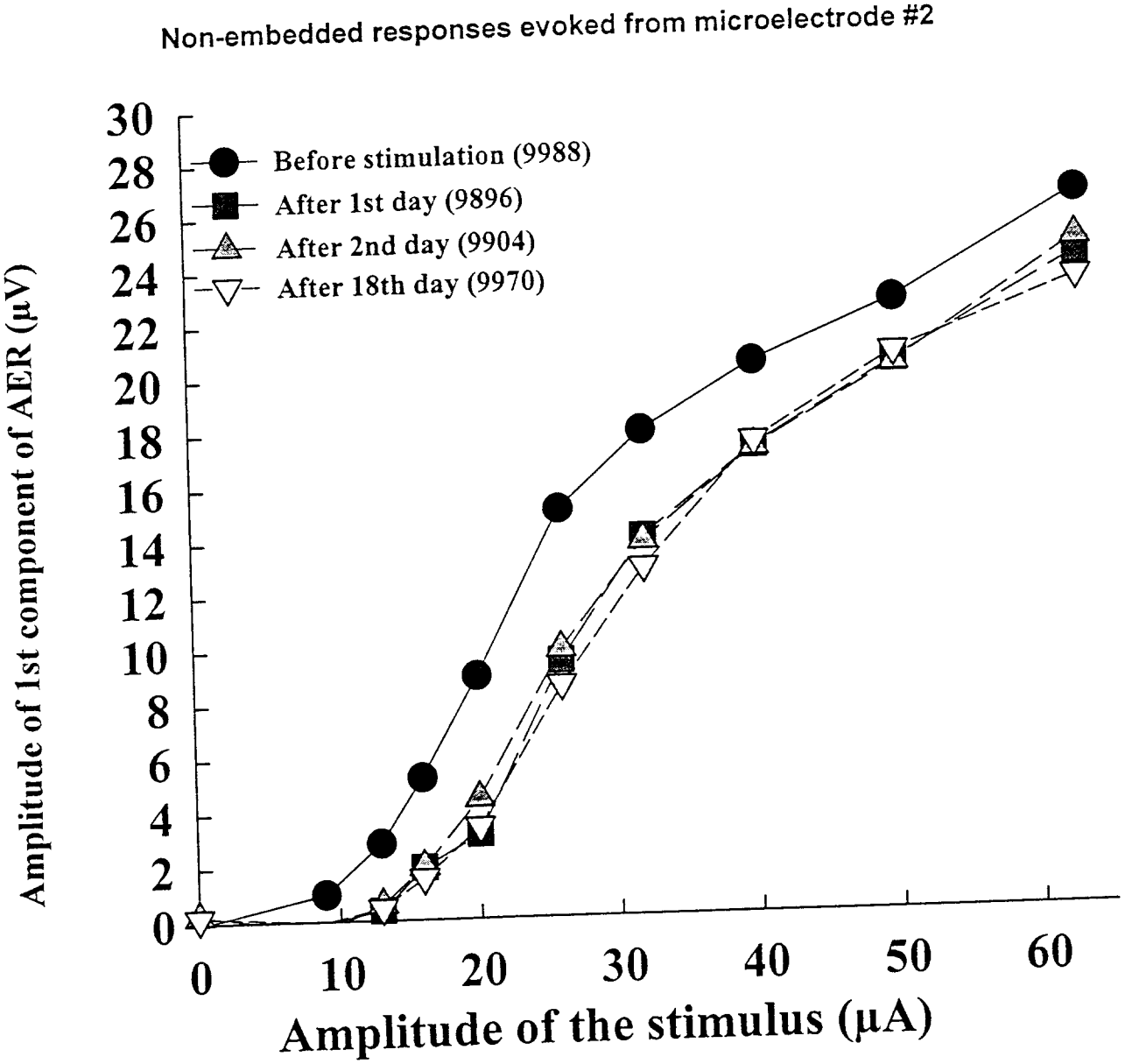

e:/spw/cn/cn133ae2.spw

Figure 11A

cat cn133
Electrodes 1,2, 4 pulsed over the range of 14-63 μA, 40 μs/phase, 250 Hz, 7 hrs/day according to log-compressed artificial voice signal, with 50% duty cycle.

Non-embedded responses evoked from microelectrode #2

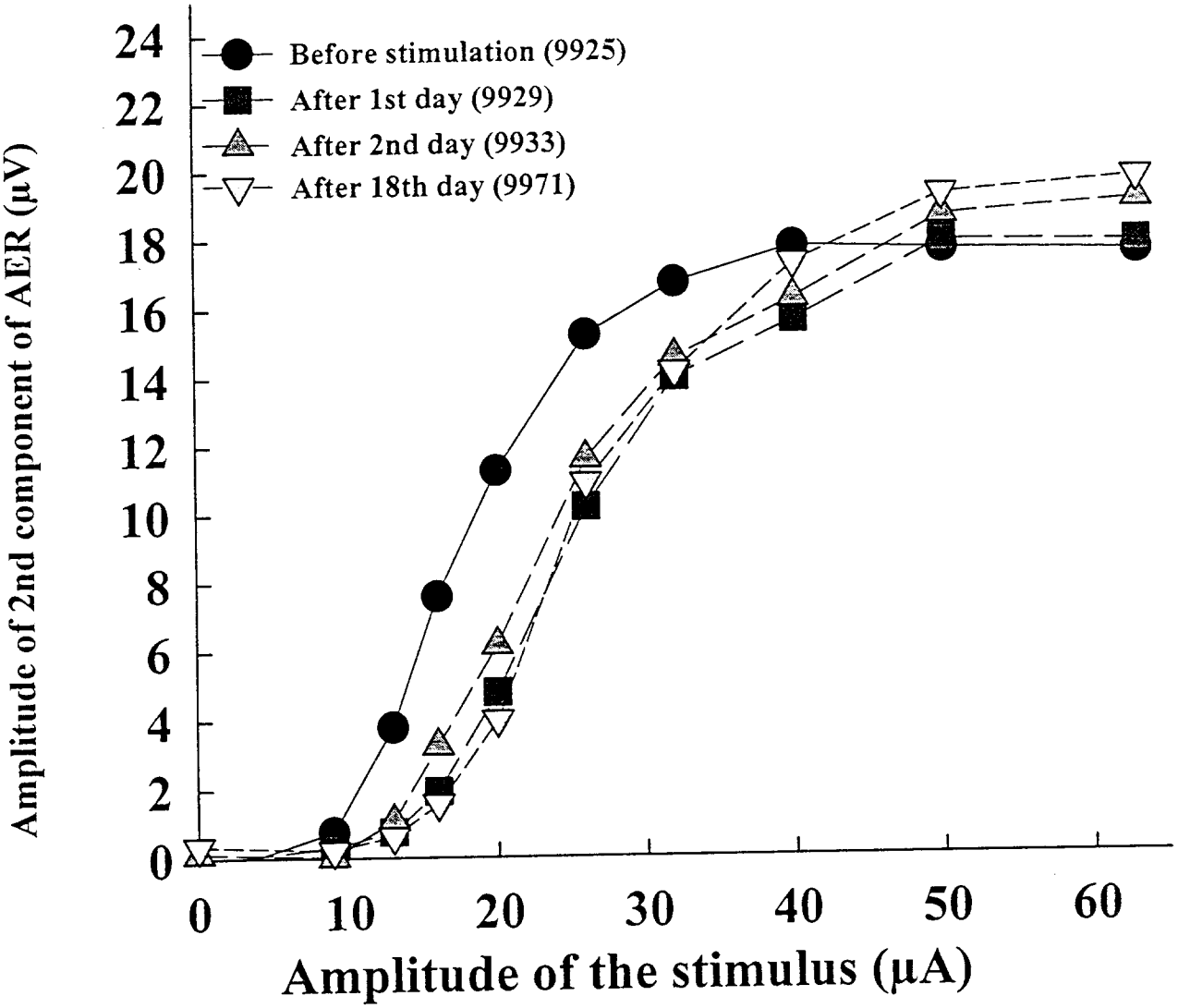

e:/spw/cn/cn133al2.spw

Figure 11B

Figure 12A: cat CN133. Tip of (pulsed) electrode #1. Bar = 100 µm

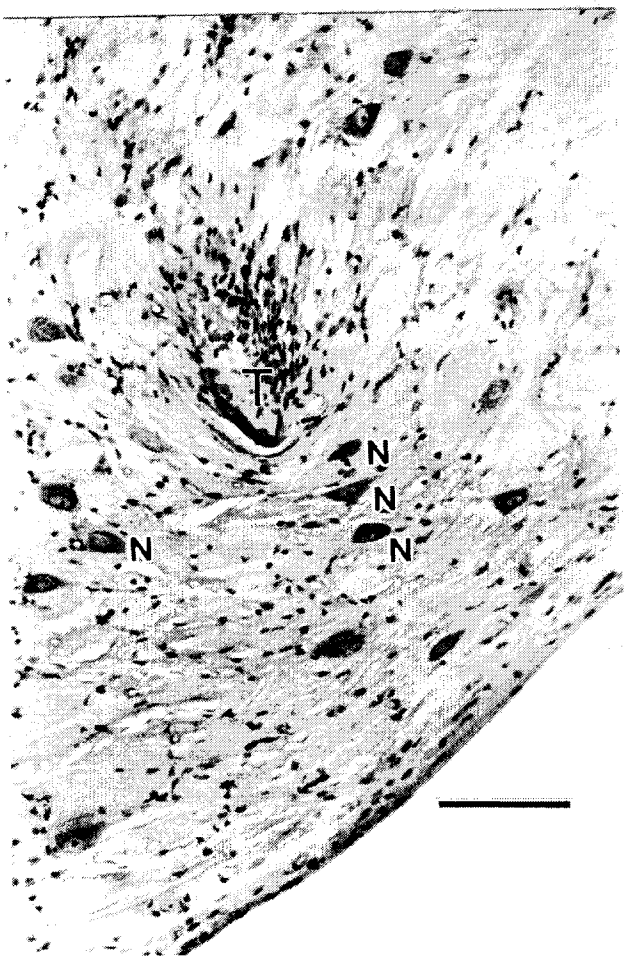

Figure 12B. cat CN133. Tip of (pulsed) electrode #2

Figure 12C: cat CN133. Tip of (unpulsed) electrode #3. Bar = 100 µm

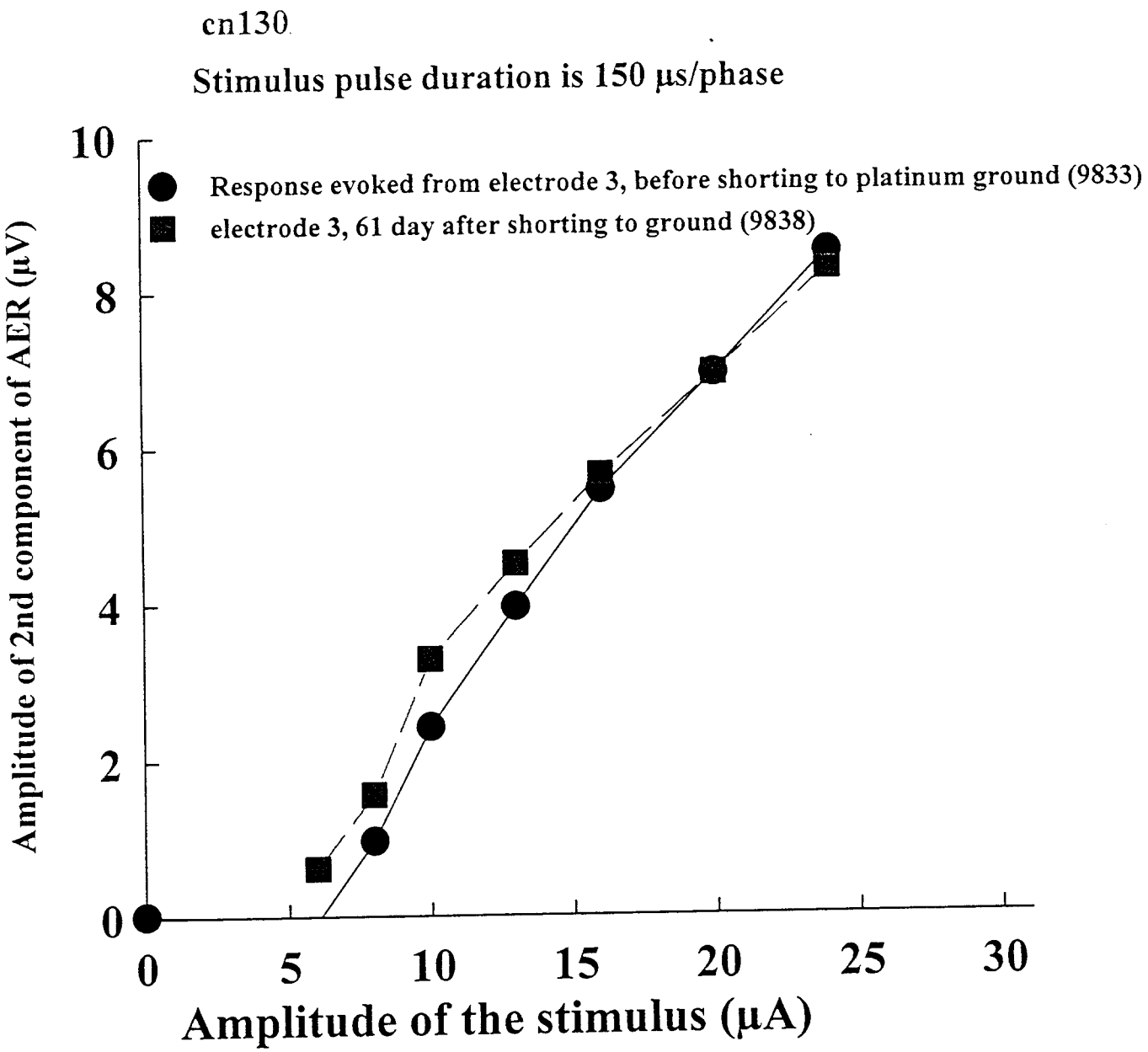

e:/spw/cn/cn130mm.spw

Figure 13